

First Missing Mass Spectroscopy of the $^{12}\text{C}(\gamma, p)$ Reaction with Simultaneous Measurement of an η' Meson

N. TOMIDA* AND LEPS2/BGOEGG COLLABORATION

*Center for Science Adventure and Collaborative Research Advancement (SACRA),
Kyoto University, Kitashirakawa-Oiwakecho, Sakyo-ku, 606-8502, Kyoto, Japan*

Doi: [10.12693/APhysPolA.142.356](https://doi.org/10.12693/APhysPolA.142.356)

*e-mail: tomida.natsuki.5z@kyoto-u.ac.jp

We carried out the first missing mass spectroscopy of the $^{12}\text{C}(\gamma, p)$ reaction with simultaneous detection of an η' meson. The experiment was performed using the BGOegg detector system at the LEPS2 beam line in SPring-8 with a 1.3–2.4 GeV photon beam. We evaluated cross-sections in different photon beam energy and different missing mass regions. The obtained cross-sections can be used to evaluate η' -nucleus optical potential from a comparison with theoretical calculations.

topics: η' meson, η' -nucleus potential, missing-mass spectroscopy

1. Introduction

Understanding the origin of hadron masses is one of the important subjects in the field of quantum chromodynamics (QCD). The chiral symmetry breaking in a vacuum plays an important role in explaining hadron masses. In a dense matter where partial restoration of chiral symmetry is expected, modifications of hadron masses can occur. There have been attempts to examine hadron masses in high density material nuclei, in both theoretical and experimental studies. The simplest way to study hadron masses in nuclei is to examine mass spectra of hadrons produced off a nuclei target. The KEK-PS E325 Collaboration reported an observation of mass modification of ϕ mesons in Cu nuclei in their e^+e^- decay [1]. The CBELSA/TAPS Collaboration studied masses of ω mesons in their $\pi^0\gamma \rightarrow 3\gamma$ decay [2]. Another way to study meson masses in nuclei is to examine meson–nucleus optical potential. According to [3], the mass shift in nuclei can be described as an attractive optical potential between the meson and the nucleus

$$U(r) = V(r) + iW(r), \quad (1)$$

$$V(r) = V_0 \frac{\rho(r)}{\rho_0} = \Delta m(\rho_0) \frac{\rho(r)}{\rho_0}, \quad (2)$$

$$W(r) = W_0 \frac{\rho(r)}{\rho_0}, \quad (3)$$

where V and W indicate the real and imaginary part of the optical potential, and r is the distance from the center of the nucleus. In (1)–(3), $\rho(r)$ and ρ_0 are the nuclear density distribution and the normal nuclear density, respectively, and $\Delta m(\rho_0)$ is the

mass shift at the normal nuclear density. The optical potential can be studied with missing mass spectroscopy around the meson production threshold. If V_0 is large and W_0 is small, the meson and the nucleus may form a bound state. A large Δm of -150 and -80 MeV of the $\eta'(958)$ meson owing to its $U_A(1)$ anomaly is expected with calculations using the Nambu–Jona–Lasinio and linear sigma models, respectively [3, 4]. A smaller Δm of -37 MeV is expected with the Quark-Meson Coupling model [5]. The η -PRiME/Super-FRS Collaboration searched for a bound state with missing mass spectroscopy of the $^{12}\text{C}(p, d)$ reactions around the η' production threshold [6, 7]. Under large multi-meson background, no bound state was observed, although they used an excellent resolution spectrometer. They derived an upper limit of V_0 and W_0 from the comparison with the theoretical calculation based on a distorted wave impulse approximation (DWIA) [8]. The CBELSA/TAPS Collaboration studied η' mesons produced off C and Nb nuclei in detail [9, 10]. They evaluated V_0 as $[-39 \pm 7(\text{stat}) \pm 15(\text{syst})]$ MeV from the comparison of the differential cross-sections with a collisional model [11]. They also measured the $\gamma + ^{12}\text{C} \rightarrow p + \eta' + X$ reaction in $2^\circ < \cos(\theta_{lab}^p) < 11^\circ$ and showed the photon beam energy dependence of the cross-section [12]. They show that the height of the bump structure around the photon beam energy of 1.6 GeV is a key to evaluating V_0 according to the collision model calculation. In [12], the proton energy was not measured, and thus missing mass spectroscopy was not carried out in their measurement. The COSY-11 Collaboration measured the $pp \rightarrow pp\eta'$ reaction and evaluated the real part of

the η' -proton scattering length as 0.00 ± 0.43 fm [13]. It corresponds to $V_0 = 0 \pm 37.9$ MeV [14]. Recent studies on η' meson are summarized in [14, 15].

To study the η' mass in nuclei, we carried out experiments at the LEPS2 beamline in SPring-8 using the BGOegg electromagnetic calorimeter. We examined the 2γ invariant mass spectra of the η' meson produced off a carbon target. The preliminary result is shown elsewhere [16]. In addition, we carried out missing mass spectroscopy of the $^{12}\text{C}(\gamma, p)$ reaction. Around the η' production threshold, there are huge background events coming from multi-meson productions. To identify events from η' production, we simultaneously measured decay products from the η' -nucleus system. We measured an η meson-proton pair, which is considered to be emitted from one nucleon absorption process of an η' meson, $\eta'N \rightarrow \eta N$, where N indicates a nucleon. After kinematical selections of η -p pairs, no events considered to be η' bound states were observed [17]. We evaluated V_0 as a function of the branching fraction of the $\eta'N \rightarrow \eta N$ process based on the comparison of the cross-sections with a calculation within DWIA [18]. In this article, we report the results of the missing mass spectroscopy with simultaneous measurement of η' mesons escaping from nuclei.

2. Experiment

We measured the $\gamma + ^{12}\text{C} \rightarrow p + \eta' + X$ reaction at the LEPS2 beamline in SPring-8 [19]. A photon beam with a tagged energy range of 1.3–2.4 GeV was derived from the backward Compton scattering of the 355 nm laser and the SPring-8 8 GeV electrons. A carbon target with 20 cm thickness was hit by 6.1×10^{12} photons. An UpVeto counter made of a 3 mm thick plastic scintillator was used to ensure that the beam photon did not convert to e^+e^- before arriving at the target. The photon beam energy was evaluated by measuring a track of a recoiled electron using a tagging counter, which consists of 1 mm-wide fiber scintillators. The photon beam energy resolution was 12 MeV. The proton energy was measured based on the time-of-flight (TOF) between the RF signal of the storage ring and the TOF wall consisting of resistive plate chambers (RPCs) [20, 21]. The RPC-TOF was located 12.5 m downstream from the target and covered the polar angle of 0.9° – 6.8° . The time resolution of the TOF was 60–90 ps, depending on the RPC hit position. The missing mass resolution was 12–30 MeV/c^2 , depending on the proton energy. The η' meson was identified from its 2γ decay process. Energies and angles of two photons were measured using the BGOegg calorimeter, consisting of 1320 BGO crystals [22]. The energy resolution of the BGOegg calorimeter was 1.4% for 1 GeV γ . The polar angle coverage of the BGOegg calorimeter was from 24° to 144° . The inner plastic scintillators (IPs) with 5 mm thickness were used for charge identification of particles measured at the BGOegg.

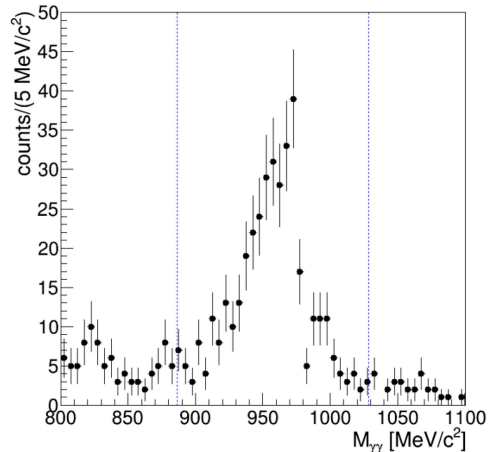


Fig. 1. The 2γ invariant mass distribution around the η' mass. The region in $\pm 4\sigma$ from the peak is indicated with the blue-dashed lines.

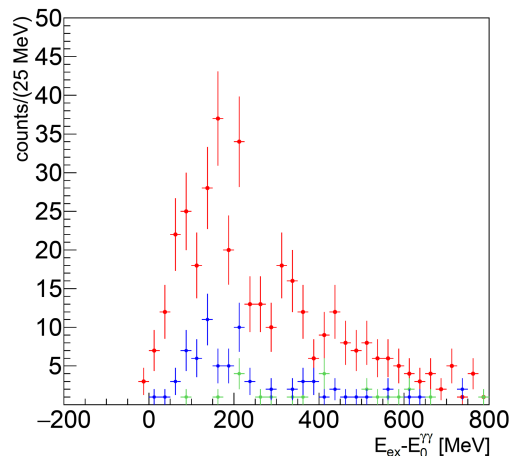


Fig. 2. The missing mass distribution of the $\gamma + ^{12}\text{C} \rightarrow p + \eta' + X$ reaction. The horizontal axis is the excitation energy, $E_{\text{ex}} - E_0^{\gamma\gamma} = MM(^{12}\text{C}(\gamma, p_f)) - M_{11\text{B}} - M_{\gamma\gamma}$. The red, blue and green histograms indicate events in $-4\sigma < M_{\gamma\gamma} < +4\sigma$, $-8\sigma < M_{\gamma\gamma} < -4\sigma$, and $+4\sigma < M_{\gamma\gamma} < +8\sigma$, respectively.

The drift chamber, located 1.6 m downstream of the target, was used to ensure that there are no charged particles other than the proton measured by the RPC-TOF in the forward polar angle region, which is not covered by BGOegg. The details of the detector setup are described in [23].

3. Analysis

We selected events in which only two photons were detected in the BGOegg, and only one charged particle at the DC and the RPC-TOF. The 2γ invariant mass, $M_{\gamma\gamma}$, around the η' mass is shown in Fig. 1. The invariant mass resolution was $17 \text{ MeV}/c^2$. We selected the region within $\pm 4\sigma$ from the peak as the signal, and $-8\sigma < M_{\gamma\gamma} < -4\sigma$

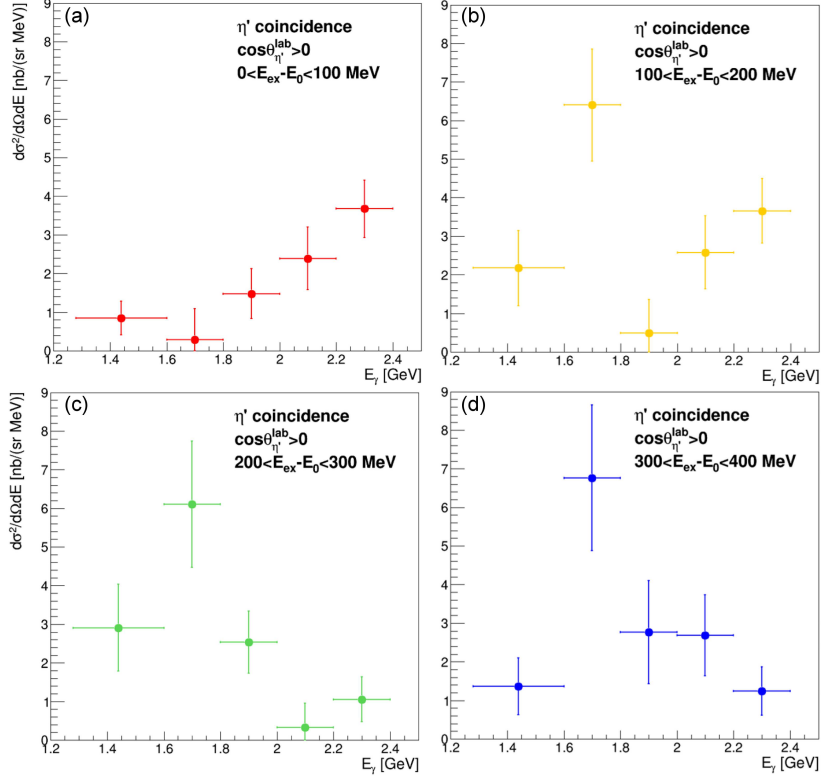


Fig. 3. The E_γ dependence of the cross-section of the $^{12}\text{C}(\gamma, p)$ reaction with simultaneous measurement of an η' meson in different $E_{\text{ex}} - E_0^{\gamma\gamma}$ region.

and $4\sigma < M_{\gamma\gamma} < 8\sigma$ as the side band. To suppress background events from the $\gamma + ^{12}\text{C} \rightarrow p + \eta' + \pi + X$ reaction, we required that the missing energy was smaller than 150 MeV. The missing energy was defined as

$$E_{\text{miss}} = E_\gamma + M_{^{12}\text{C}} - M_{^{11}\text{B}} - E_{\gamma_1} - E_{\gamma_2} - E_p, \quad (4)$$

where $M_{^{12}\text{C}}$ and $M_{^{11}\text{B}}$ represent the masses of ^{12}C and ^{11}B nuclei, and $E_\gamma, E_{\gamma_1}, E_{\gamma_2}$, and E_p represent the energies of the photon beam, the photons detected with BGOegg, and the proton detected with the RPC-TOF, respectively. The missing mass spectra of the signal and side band region are shown in Fig. 2. The red, blue, and green histograms indicate events in $-4\sigma < M_{\gamma\gamma} < +4\sigma$, $-8\sigma < M_{\gamma\gamma} < -4\sigma$, and $+4\sigma < M_{\gamma\gamma} < +8\sigma$, respectively. The horizontal axis is the excitation energy defined as

$$E_{\text{ex}} - E_0^{\gamma\gamma} = MM(^{12}\text{C}(\gamma, p_f)) - M_{^{11}\text{B}} - M_{\gamma\gamma}, \quad (5)$$

where $MM(^{12}\text{C}(\gamma, p_f))$ is the missing mass in the $^{12}\text{C}(\gamma, p_f)$ reaction. The excitation energy, $E_{\text{ex}} - E_0^{\gamma\gamma} = 0$ MeV, corresponds to the η' production threshold. A clear missing mass distribution rising from the production threshold was observed. We used $M_{\gamma\gamma}$ instead of the mass of the η' meson so that $E_{\text{ex}} - E_0^{\gamma\gamma} = 0$ MeV would be the production threshold of corresponding $\gamma\gamma$ events even for side band events of $M_{\gamma\gamma}$.

We evaluated cross-sections in every 100 MeV excitation energy bin and in five photon beam energy bins. We deduced the detector acceptance as a function of the η' kinetic energy and polar angle using a Monte Carlo (MC) simulation based on GEANT4 [24]. The $\gamma + p \rightarrow \eta' + p$ reaction was implemented into the simulation, taking into account the Fermi motion. We evaluated the cross-section in $\cos(\theta_{lab}^{\eta'}) > 0$. The number of events observed in $\cos(\theta_{lab}^{\eta'}) < 0$ was the same for the signal and sideband regions and the events observed in $\cos(\theta_{lab}^{\eta'}) < 0$ likely come from the combinatorial background. We deduced acceptance event by event using the measured kinetic energy and polar angle. The cross-section of side band events was subtracted in each bin. The systematic uncertainty of the cross-section was evaluated to be 6.7%. It comes from the uncertainty of the number of incident photons (1.3%), the number density of the target (1.1%), the detector reconstruction efficiencies (5.2%), the contamination of pions to the forward-going proton (1.4%), and the branching fraction of the $\eta' \rightarrow 2\gamma$ mode (3.6%).

4. Results

In Fig. 3, we show the photon beam energy (E_γ) dependence of the cross-sections in the laboratory (Lab) frame in different $E_{\text{ex}} - E_0^{\gamma\gamma}$ regions. The overall cross-section is consistent with

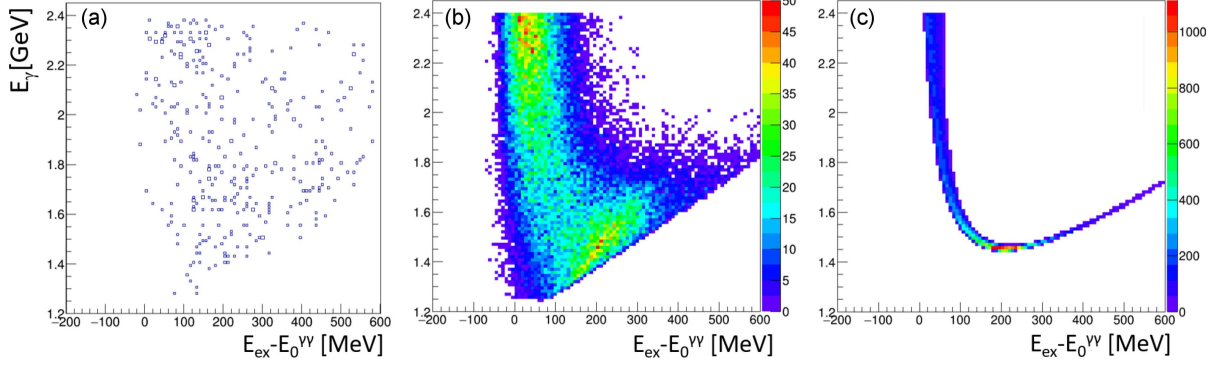


Fig. 4. The two-dimensional event distributions of E_γ and $E_{\text{ex}} - E_0^{\gamma\gamma}$. Here, (a) presents the experimental data, (b) MC simulation data with Fermi motion, and (c) MC data with a proton target.

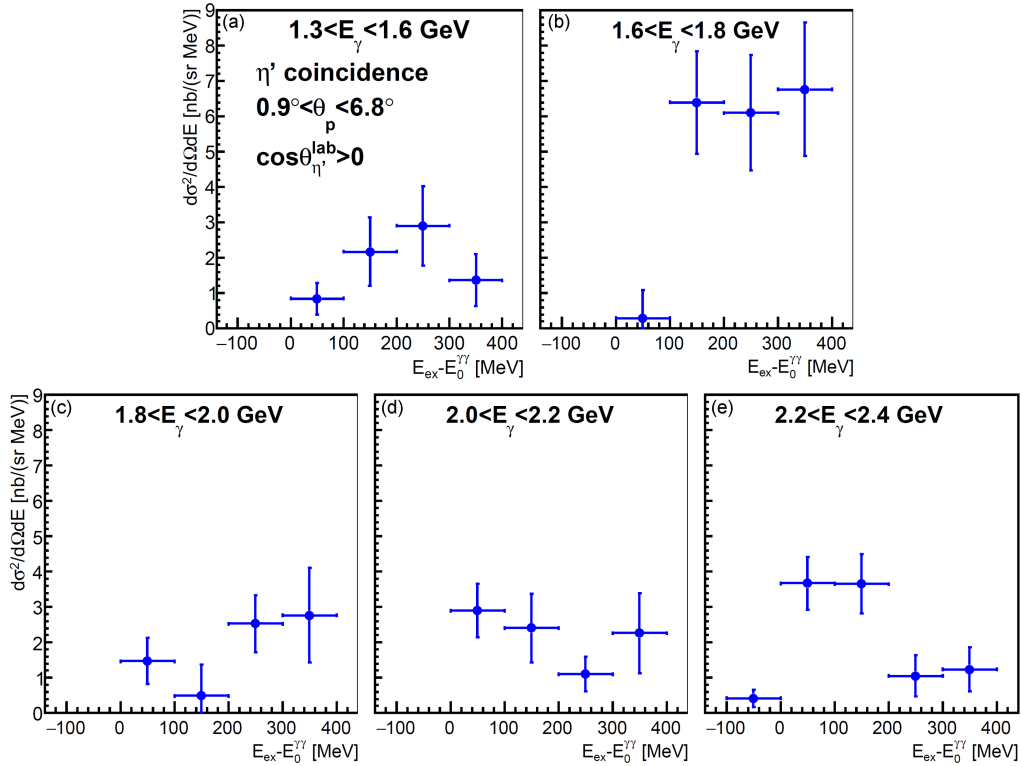


Fig. 5. The missing mass distribution of the $^{12}\text{C}(\gamma, p)$ reaction with simultaneous measurement of an η' meson in different E_γ regions.

the measurement by the CBELSA/TAPS Collaboration in [12], although the polar angle acceptance for protons is slightly different. The bump around $E_\gamma = 1.6$ GeV observed in [12] was observed in $100 \text{ MeV} < E_{\text{ex}} - E_0^{\gamma\gamma}$ but not in $E_{\text{ex}} - E_0^{\gamma\gamma} < 100 \text{ MeV}$. The reason for this becomes clear when we compare event distributions in two-dimensional plots of E_γ and $E_{\text{ex}} - E_0^{\gamma\gamma}$ of the experimental signal data (a), MC data with target Fermi motion (b), and MC data with a proton target (c) in Fig. 4. The MC data was produced assuming a constant cross-section of the elementary $\gamma + p \rightarrow \eta' + p$ reaction in the center-of-mass (CM) system, the E_γ distribution of the laser electron photon, and the acceptance

of the detector system. The event concentration around $E_\gamma = 1.5$ GeV in Fig. 4c comes from a large transformation factor of the cross-section from the CM to the Lab frame in our detector setup, where the proton is detected at very forward angles. Figure 3b indicates that the CM \rightarrow Lab transformation factor plays an important role in the E_γ distribution even with a nuclear target. In $E_{\text{ex}} - E_0^{\gamma\gamma} < 100 \text{ MeV}$, there is a small E_γ dependence of the transformation factor, and thus the bump was not observed. It would be interesting to compare the E_γ dependence of the cross-sections in different $E_{\text{ex}} - E_0^{\gamma\gamma}$ regions with the collisional model [11, 12] to evaluate V_0 .

Figure 5 shows the $E_{\text{ex}} - E_0^{\gamma\gamma}$ distributions in different photon beam energies. We can see that the distribution is different for different E_γ . This is the first missing mass spectroscopy around the η' threshold detecting an η' meson simultaneously. This data can be used to evaluate the η' -nucleus potential from the comparison with DWIA calculations calculated up to large $E_{\text{ex}} - E_0^{\gamma\gamma}$. In the case of Σ hyper nuclei, V_0 is evaluated based on the comparison of E_{ex} distributions of experimental data of quasi-free process and theoretical calculations within the DWIA calculated up to $E_{\text{ex}} - E_0 \simeq 200$ MeV [25, 26].

5. Conclusions

We carried out the missing mass spectroscopy of the $^{12}\text{C}(\gamma, p)$ reaction with simultaneous measurement of an η' meson. The cross-sections in different missing mass and photon beam energy regions are reported for the first time. This data can be used for evaluating the η' -nucleus potential based on the comparison with theoretical calculations.

Acknowledgments

The experiment was performed at the BL31LEP beam line of SPring-8 with the approval of the Japan Synchrotron Radiation Research Institute (JASRI) as a contract beam line (Proposal No. BL31LEP/6101). This research was supported in part by the Ministry of Education, Culture, Sports, Science and Technology of Japan (MEXT) Scientific Research on Innovative Areas Grant No. JP21105003, No. JP24105711 and No. JP18H05402, Japan Society for the Promotion of Science (JSPS) Grant-in-Aid for Specially Promoted Research Grant No. JP19002003, Grant-in-Aid for Scientific Research (A) Grant No. JP24244022, Grant-in-Aid for Young Scientists (A) Grant No. JP16H06007, Grant-in-Aid for Scientific Research (C) Grant No. JP19K03833, Grants-in-Aid for JSPS Fellows No. JP24608, the National Research Foundation of Korea Grant No. 2017R1A2B2011334, and the Ministry of Science and Technology of Taiwan.

References

- [1] R. Muto, J. Chiba, H. En'yo et al., *Phys. Rev. Lett.* **98**, 042501 (2007).
- [2] M. Nanova, V. Metag, G. Anton et al., *Phys. Rev. C* **82**, 035209 (2010).
- [3] H. Nagahiro, M. Takizawa, S. Hirenzaki, *Phys. Rev. C* **74**, 045203 (2006).
- [4] S. Sakai, D. Jido, *Phys. Rev. C* **88**, 064906 (2013).
- [5] S.D. Bass, A.W. Thomas, *Phys. Lett. B* **634**, 368 (2006).
- [6] Y.K. Tanaka, K. Itahashi, H. Fujioka et al., *Phys. Rev. Lett.* **117**, 202501 (2016).
- [7] Y.K. Tanaka, K. Itahashi, H. Fujioka et al., *Phys. Rev. C* **97**, 015202 (2018).
- [8] H. Nagahiro, D. Jido, H. Fujioka, K. Itahashi, S. Hirenzaki, *Phys. Rev. C* **87**, 045201 (2013).
- [9] M. Nanova, V. Metag, E. Paryev et al., *Phys. Lett. B* **727**, 417 (2013).
- [10] M. Nanova, S. Friedrich, V. Metag et al., *Phys. Rev. C* **94**, 025205 (2016).
- [11] E.Y. Paryev, *J. Phys. G Nucl. Part. Phys.* **40**, 025201 (2013).
- [12] M. Nanova, S. Friedrich, V. Metag et al., *Eur. Phys. J. A* **54**, 182 (2018).
- [13] E. Czerwiński, P. Moskal, M. Silarski et al., *Phys. Rev. Lett.* **113**, 062004 (2014).
- [14] S.D. Bass, V. Metag, P. Moskal, [arXiv:2111.01388](https://arxiv.org/abs/2111.01388) (2021).
- [15] S.D. Bass, P. Moskal, *Rev. Mod. Phys.* **91**, 015003 (2019).
- [16] N. Tomida, “Study of the η' meson in nuclei in the LEPS2/BGOegg experiment” in: 4th Jagiellonian Symposium on Advances in Particle Physics and Medicine, 2022.
- [17] N. Tomida, N. Muramatsu, M. Niyama et al., *Phys. Rev. Lett.* **124**, 202501 (2020).
- [18] H. Nagahiro, *JPS Conf. Proc.* **13**, 010010 (2017).
- [19] N. Muramatsu, M. Yosoi, T. Yorita et al., *Nucl. Instrum. Methods A* **1033**, 166677 (2022).
- [20] N. Tomida, N. Tran, M. Niyama, M. Niyama, H. Ohnishi, C.-Y. Hsieh, M.-L. Chu, W.-C. Chang, J.-Y. Chen, Y. Matsumura, K. Shiraishi, *J. Instrum.* **9**, C10008 (2014).
- [21] N. Tomida, N. Tran, M. Niyama, H. Ohnishi, N. Muramatsu, *J. Instrum.* **11**, C11037 (2016).
- [22] T. Ishikawa, H. Fujimura, D. Grigoriev et al., *Nucl. Instrum. Methods Phys. Res. A* **837**, 109 (2016).
- [23] N. Muramatsu, J.K. Ahn, W.C. Chang et al., *Phys. Rev. C* **100**, 055202 (2019).
- [24] S. Agostinelli, J. Allison, K. Amako et al., *Nucl. Instrum. Methods Phys. Res. A* **506**, 250 (2003).
- [25] T. Harada, Y. Hirabayashi, *Nucl. Phys. A* **759**, 143 (2005).
- [26] T. Harada, R. Honda, Y. Hirabayashi, *Phys. Rev. C* **97**, 024601 (2018).